Investigation of the Dose Properties and Source to Source Variabilities in Xoft Source

Azin Esmaelbeigi[1,2], Jonathan Kalinowski[1,2], Te Vuong[2], Shirin A. Enger[1,2]

[1]Medical Physics Unit, Department of Oncology, Faculty of Medicine, McGill University, Montréal, Québec, Canada
[2]Lady Davis Institute for Medical Research, Jewish General Hospital, Montréal, Québec, Canada

Introduction

- The Xoft® Axxent® Electronic Brachytherapy System® is an effective treatment for the early-stage endorectal adenocarcinoma, specifically for tumors up to 3 cm in diameter and within 10 cm from the rectal opening.
- It utilizes a low-energy X-ray source with an average energy of around 26 keV, initially characterized in 2006 [1].
- Subsequent modifications by the manufacturer included adding a plastic anode-centering insert, which resulted in the work by Hiatt et al., 2015 [2].
- As shown in [2], the deviations in source design can impact dose rates by over 2%, exceeding standards as recommended by TG-156 [3]. Moreover, variations in elemental composition, particularly close to the anode, contribute to spectral differences among sources of the same model. In 2022, the manufacturer provided different thickness values for an Ag layer and distinct epoxy material.
- Due to the sources of uncertainty in the manufacturing of the source, accurate modeling and a robust pipeline is crucial to obtain precise x-ray spectra and dose distributions.
- Given these factors, our research focuses on creating the pipeline to characterize the Xoft electronic brachytherapy source dosimetry and beam quality and circumvent the uncertainties due to source-to-source differences. We aim to establish a systematic approach by creating a simulation and measurement pipeline for characterizing the dosimetric and spectrometric properties of the Xoft source.

Materials and Methods

- A software called E-Brachy, a Monte Carlo-based dose calculation software package, was developed using the Geant4 Monte Carlo toolkit.
- **First the source was prepared:**

1. Geometry and material descriptions for the Xoft electronic brachytherapy source were obtained in CAD format from Xoft
2. CAD files were converted to GDML format using GUIMesh, a Python-based tool.
3. Material composition and mass densities were assigned to source geometry parts.

- **Monte Carlo simulation in the E-Brachy consisted of two parts:**

1. Simulations start with electrons as primary particles, generating x-rays upon anode bombardment. Various x-ray characteristics are scored and saved in a phase space file.
2. The phase space file is used to investigate interactions between x-rays and applicators/detectors/patients.

- **In the second part of the simulations:**

1. The energy fluence spectrum of the generated x-rays 178 cm from the origin of the source was investigated for various material compositions that were provided by the vendor and were compared to the measured spectra at NIST at the similar distance
2. beam half value layer of the beam generated by the source was investigated by adding layers of Al in the simulation environment 50 cm from the source in air, calculating the resulting air kerma, and observing when the value drops to the 50% of the value without layers of Al
3. To calculate dosimetric properties of the source, the volume around the source was cylindrically parametrized with concentric cylindrical shells sectioned in Z and ρ directions and simulated three times with varying section sizes of dρ=dZ=0.01 cm at 0<ρ<1cm , dρ=dZ=0.05 cm at 0<ρ<5cm, dρ=dZ=0.1cm at 0<ρ<10cm and dρ=dZ=0.2 cm at 0<ρ<20cm as per suggested by Taylor et al., 2007 [6].

Results and Discussion

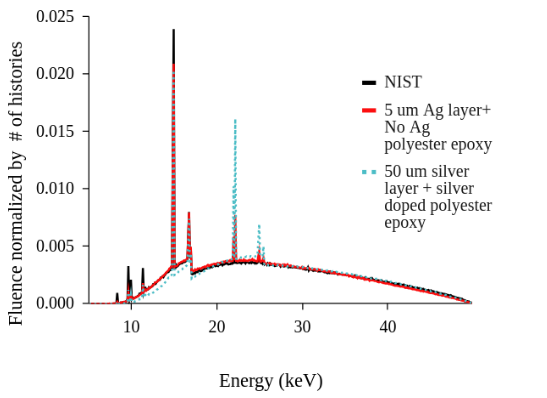

Figure 1. Depicts the spectra measured by NIST (black line), with thin layer of Ag at the wall around the vacuum of the source and a polyester epoxy (red line) and a thicker Ag wall and a silver doped epoxy (blue dashed line)

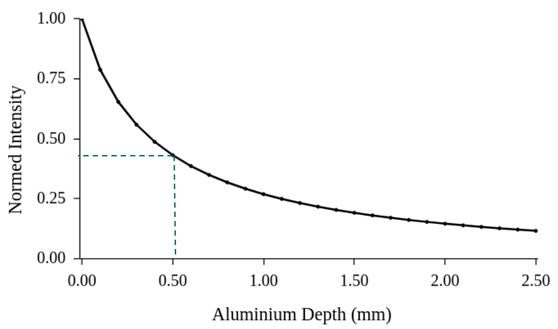

Figure 2. The relative air kerma (relative intensity normalized by maximum value) vs. Al thickness at 50 cm from the source origin is depicted. The beam half value layer for this source was calculated to be 0.434 mm ± 0.1%.

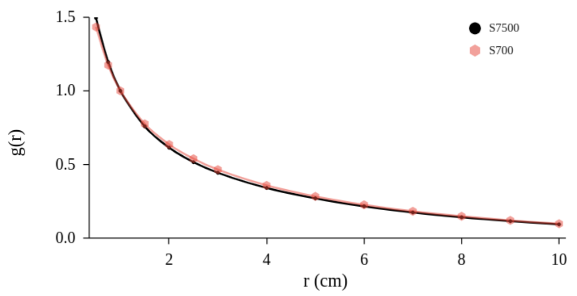

Figure 3. Shows the radial dose function versus the distance from the source model we received from the vendor (S7500) which is shown in black and the older model (S700) in red.

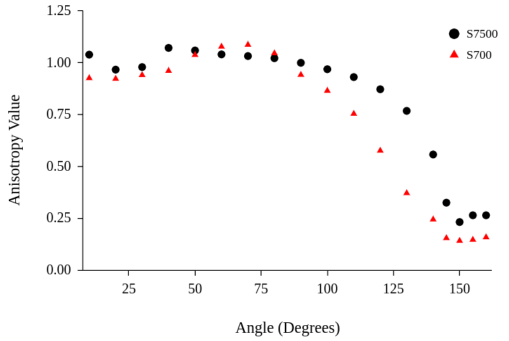

Figure 4. Shows the anisotropy functions vs. Polar angle at 1cm from the source for the model we received from the vendor (S7500) which is shown in black and the older model (S700) in red.

- **Material Composition Uncertainties:** In the material composition of the source provided by the vendor, there were uncertainties. These uncertainties encompassed factors such as the level of Ag used in the epoxy surrounding the anode and the thickness of the Ag wall that encased the x-ray source's vacuum. To resolve these uncertainties, different material compositions were compared. Ultimately, the material composition that closely matched NIST measurements (the red line) was selected for generating x-rays in the initial simulations.
- **Beam Half Value Layer (HVL):** The beam half value layer (HVL) was measured at 0.434, with a deviation of ±0.1%. This measurement provides crucial information about the beam quality.
- **Comparison Between Models S7500 and S700:** Despite minimal reported differences between models S7500 (the received model) and S700 (the previous model) by the vendor, studies by Hiat et al. in 2015 [2] revealed that the geometry and material compositions of sources, even within the same model, had undergone changes. Moreover, due to the small size and manufacturing limitations, certain parts of the source are manually handled. Consequently, a comparison of dosimetric properties between models S7500 and S700 was conducted. Although both models exhibited similar radial dose functions (figure 3) , they displayed discrepancies in their anisotropy patterns (figure 4.)
- **Table 2: Summary of S7500 vs. S700 Ratios:** In Table 2, a summary of ratios between model S7500 and S700 is presented. The values highlighted within green boxes represent ratios lower than 1.13, while the red boxes emphasize ratios higher than 1.5. This comparison indicates that anisotropy functions diverge more significantly at lower distances but converge as the distance from the sources increases.

Table 1: Includes the anisotropy function values at different distances and polar angles

$\theta°/r(\mathrm{cm})$	0.5	1	1.5	2	3	5	7	10
10	0.7973	1.0394	1.0239	1.0635	1.1074	1.1504	1.1602	1.1900
20	0.8172	0.9670	1.0314	1.0672	1.1050	1.1398	1.1529	1.1813
30	0.8489	0.9793	1.0299	1.0577	1.1050	1.1209	1.1321	1.1582
40	-	1.0719	1.0950	1.1066	1.1186	1.1327	1.1375	1.1515
50	0.9960	1.0595	1.0825	1.0934	1.1039	1.1144	1.1192	1.1293
60	0.9759	1.0406	1.0625	1.0729	1.0829	1.0902	1.0924	1.1010
70	0.9886	1.0325	1.0494	1.0549	1.0608	1.0647	1.0659	1.0700
80	1.0001	1.0222	1.0292	1.0325	1.0340	1.0338	1.0351	1.0375
90	1.0000	1.0000	1.0000	1.0000	1.0000	1.0000	1.0000	1.0000
100	0.9900	0.9690	0.9660	0.9645	0.9627	0.9623	0.9607	0.9596
110	0.9775	0.9311	0.9239	0.9207	0.9183	0.9171	0.9161	0.9110
120	0.9489	0.8723	0.8639	0.8607	0.8591	0.8591	0.8592	0.8547
130	0.8780	0.7680	0.7554	0.7534	0.7601	0.7690	0.7718	0.7724
140	-	0.5575	0.5628	0.5790	0.6026	0.6264	0.6364	0.6542
145	-	0.3250	0.3792	0.4271	0.4625	0.5157	0.5347	0.5760
150	-	0.2316	0.2951	0.3331	0.3643	0.4294	0.4521	0.5079
155	-	0.2642	0.3641	0.3307	0.3521	0.4112	0.4335	0.4829
160	-	-	0.4147	0.3399	0.3517	0.4058	0.4253	0.4747
165	-	-	0.4688	0.3565	0.3634	0.4130	0.4339	0.4766
170	-	-	0.6290	0.4834	0.4705	0.4982	0.5070	0.5256
175	-	-	2.2576	1.2698	0.8765	0.6996	0.6624	0.6077

Table 2: Indicates the anisotropy function ratio between the more recent Xoft source model (S7500) and the older version (S700) at different distances and polar angles

$\theta°/r(\mathrm{cm})$	0.5	1	1.5	2	3	5	7	10
10	0.9807	1.1261	1.0502	1.0572	1.0628	1.0652	1.0557	1.0673
20	0.9846	1.0276	1.0439	1.0504	1.0544	1.0535	1.0481	1.0566
30	0.9581	1.0191	1.0361	1.0420	1.0604	1.0427	1.0357	1.0416
40	-	1.0327	1.0330	1.0313	1.0290	1.0269	1.0220	1.0236
50	0.9604	0.9828	0.9922	0.9958	1.0008	1.0039	1.0029	1.0056
60	0.9232	0.9573	0.9712	0.9780	0.9862	0.9902	0.9895	0.9937
70	0.9309	0.9871	0.9725	0.9777	0.9840	0.9876	0.9878	0.9898
80	0.9616	1.0851	0.9830	0.9871	0.9895	0.9902	0.9915	0.9938
90	1	1	1	1	1	1	1	1
100	1.0432	1.1203	1.0243	1.0217	1.0177	1.0151	1.0134	1.0122
110	1.1095	1.2349	1.0632	1.0534	1.0435	1.0362	1.0316	1.0282
120	1.2213	1.5145	1.1338	1.1163	1.0944	1.0725	1.0647	1.0565
130	1.5270	2.0700	1.2569	1.2112	1.1659	1.1226	1.1010	1.0863
140	-	2.2848	1.3497	1.2839	1.2101	1.1369	1.0992	1.0940
145	-	2.1102	1.2474	1.2345	1.1449	1.0972	1.0567	1.0787
150	-	1.6424	1.4393	1.3540	1.1829	1.1125	1.0489	1.0852
155	-	1.8094	1.9680	1.4896	1.2530	1.1617	1.0919	1.1177
160	-	-	2.2783	1.5809	1.3075	1.2041	1.1280	1.1577
165	-	-	2.6635	1.7474	1.4196	1.2867	1.2088	1.2190
170	-	-	3.9071	2.6414	2.0107	1.6495	1.4825	1.4054
175	-	-	-	-	4.1539	2.5350	2.0830	1.7166

Conclusion

- Developed a Monte Carlo dosimetry package for electronic brachytherapy.
- Optimized the package's performance.
- Calculated the source spectrum with various material compositions.
- Selected the composition closest to NIST experimental measurements.
- Found the beam's half-value layer to be 0.434 mm + 0.1% Aluminum at 50 cm from the source in air.
- Compared dosimetry of the received model (S7500) with a previously studied one [2].
- Noted that radial dose functions matched, but anisotropy function discrepancies increased at higher angles and shorter distances from the source in the two models.

References

[1] M. J. Rivard, S. D. Davis, L. A. DeWerd, T. W. Rusch, and S. Axelrod, "Calculated and measured brachytherapy dosimetry parameters in water for the Xoft Axxent X-ray source: An electronic Brachytherapy Sources)," Medical Physics, vol. 33, no. 11, pp. 4020–4032, 2006.
[2] J. Hiatt, S. Davis, and M. Rivard, "A revised dosimetric characterization of the Model S700 Electronic Brachytherapy source containing an anode-centering plastic insert and other components not included in the 2006 model," Medical Physics, vol. 42, no. 6Part1, pp. 2764–2776, 2015.
[3] R. Nath, L. L. Anderson, J. A. Meli, A. J. Olch, J. A. Stitt, and J. F. Williamson, "Code of practice for brachytherapy physics: Report of the AAPM Radiation Therapy Committee Task Group No. 56," Medical Physics, vol. 24, no. 10, pp. 1557–1598, 1997.
[4] Agostinelli, S., et al. "Geant4—a Simulation Toolkit." Nuclear Instruments and Methods in Physics Research Section A: Accelerators, Spectrometers, Detectors and Associated Equipment, vol. 506, no. 3, 2003, pp. 250–303., doi:10.1016/s0168-9002(03)01368-8.
[5] M. Pinto and P. Gonçalves, "Guimesh: A tool to import step geometries into GEANT4 via GDML," Computer Physics Communications, vol. 239, pp. 150–156, 2019.
[6] Taylor, R. E., et al. "Benchmarking Brachy dose: Voxel Based EGSNRC Monte Carlo Calculations of TG-43 Dosimetry Parameters." Medical Physics, vol. 34, no. 2, 2007, pp. 445–457., doi:10.1118/1.2400843.

Acknowledgements

CIHR IRSC
TRANSMEDTECH
compute canada
Chaires de recherche du Canada
Canada Research Chairs
Canada